Organometallics 1993, *12*, 417–427

1,3-Dipolar Cycloaddition to the Fe–N=C Fragment. 8.[1] Formation of 1,4,3a,6a-Tetrahydropyrrolo[3,2-*b*]pyrroles via Double 1,3-Dipolar Cycloaddition of Alkynes to $Fe(CO)_2(CNR)(\alpha\text{-diimine})$. Competition between Isocyanide and CO Insertion. Determination of Cone Angles of Isocyanides

Paul P. M. de Lange, Hans-Werner Frühauf,* Marco J. A. Kraakman,
Maarten van Wijnkoop, Mirko Kranenburg, Arthur H. J. P. Groot, and
Kees Vrieze

Laboratorium voor Anorganische Chemie, J. H. van 't Hoff Instituut, Universiteit van Amsterdam,
Nieuwe Achtergracht 166, 1018 WV Amsterdam, The Netherlands

Jan Fraanje, Yuanfang Wang, and Milco Numan

Laboratorium voor Kristallografie, J. H. van 't Hoff Instituut, Universiteit van Amsterdam,
Nieuwe Achtergracht 166, 1018 WV Amsterdam, The Netherlands

Received August 10, 1992

$Fe(CO)_2(CNR)(R'\text{-}\alpha\text{-diimine})$ (**1** R′ = isopropyl, R = *tert*-butyl (**a**), *sec*-butyl (**b**), benzyl (**c**), cyclohexyl (**d**), *o*-tolyl (**e**), and 2,6-xylyl (**f**); **1g** R′ = cyclohexyl, R = *tert*-butyl) reacts with dimethyl acetylenedicarboxylate, via a 1,3-dipolar cycloaddition to the Fe–N=C fragment, to give three products. The first two products, ferra [2.2.2] bicyclic structures (**7**, **8**), are the result of a competition between CO and isocyanide insertion. The trend for preferred insertion proved to be aromatic CNR > CO > aliphatic CNR. The third product, a 1,4,3a,6a-tetrahydropyrrolo[3,2-*b*]pyrrole complex (**4**), is formed via two successive 1,3-dipolar cycloadditions to both Fe—N=C fragments of **1**. The distribution of products is governed by the electronic properties of the isocyanides. The pyrrolopyrrole group can be decomplexed by means of substitution by CO. Heating of the uncoordinated heterocycle results in ring cleavage, yielding 1-isopropyl-2,3-dicarbomethoxy-5-(1,2-dicarbomethoxy-2-(isopropylamino)ethenyl)pyrrole (**10**). The molecular structure of **10** ($C_{20}H_{28}N_2O_8$, monoclinic, space group $P2_1/n$, $a = 8.442$ (6) Å, $b = 29.240$ (7) Å, $c = 9.567$ (9) Å, $\beta = 109.797$ (8)°, $Z = 4$, $R = 0.059$, $R_w = 0.083$) shows that the π systems of the pyrrole and enamine units are not in conjugation. To evaluate the steric properties of isocyanide ligands, the cone angles have been determined. The approach of the nearby and remote cone angle is introduced and discussed as a means to account for the influence of the isocyano carbon atom on the steric properties.

Introduction

One of the fascinating aspects of the chemistry of transition-metal α-diimine complexes is the ease with which the imine fragment can undergo C–C,[2] C–H,[3] C–N,[4] and N–H[5] coupling reactions with a wide variety of molecules such as α-diimines,[3–7] carbodiimides,[7] sulfines,[7] ketenes,[8] and especially alkynes.[9]

In previous papers[10] we have presented the reaction between $Fe(CO)_3(R'\text{-DAB})$[11a] (**1**) and electron-deficient alkynes. In the initial step, which can be described as an oxidative 1,3-dipolar cycloaddition, the alkyne adds across

---

* To whom correspondence should be addressed.

[1] (a) Part 7: van Wijnkoop, M.; de Lange, P. P. M.; Frühauf, H.-W.; Vrieze, K.; Wang, Y.; Goubitz, K.; Stam, C. H. *Organometallics* **1992**, *11*, 3607. (b) Part 6: de Lange, P. P. M.; Frühauf, H.-W.; van Wijnkoop, M.; Vrieze, K.; Wang, Y.; Heijdenrijk, D.; Stam, C. H. *Organometallics* **1990**, *9*, 1691.

[2] (a) Staal, L. H.; Polm, L. H.; Balk, R. W.; van Koten, G.; Vrieze, K.; Brouwers, A. M. F. *Inorg. Chem.* **1980**, *19*, 3343. (b) Polm, L. H.; Elsevier, C. J.; van Koten, G.; Ernsting, J. M.; Stufkens, D. J.; Vrieze, K.; Andrea, R. R.; Stam, C. H. *Organometallics* **1987**, *6*, 1096.

[3] (a) Keijsper, J.; Grimberg, P.; van Koten, G.; Vrieze, K.; Christophersen, M.; Stam, C. H. *Inorg. Chim. Acta* **1985**, *102*, 29. (b) Zoet, R.; van Wijnkoop, M.; Versloot, P.; van Koten, G.; Vrieze, K.; Duineveld, C. A. A.; Elsevier, C. J.; Goubitz, K.; Heijdenrijk, D.; Stam, C. H.; *Organometallics* **1989**, *8*, 23.

[4] (a) Muller, F.; van Koten, G.; Vrieze, K.; Heijdenrijk, D.; Krijnen, B. B.; Stam, C. H. *Organometallics* **1989**, *8*, 41. (b) Frühauf, H.-W.; Landers, A.; Goddard, R. J.; Krüger, C. *Angew. Chem.* **1978**, *90*, 56. (c) Staal, L. H.; Polm, L. H.; Vrieze, K. *Inorg. Chim. Acta* **1980**, *40*, 165.

[5] Keijsper, J.; Mul, J.; van Koten, G.; Vrieze, K.; Ubbels, M. C.; Stam, C. H. *Organometallics* **1984**, *3*, 1732.

[6] (a) Staal, L. H.; Oskam, A.; Vrieze, K.; Roosendaal, E.; Schenk, H. *Inorg. Chem.* **1979**, *18*, 1634. (b) Keijsper, J.; van Koten, G.; Vrieze, K.; Zoutberg, M. C.; Stam, C. H. *Organometallics* **1985**, *4*, 1306. (c) van Koten, G.; Jastrzebski, J. T. B. H.; Vrieze, K. *J. Organomet. Chem.* **1983**, *250*, 49. (d) Staal, L. H.; Polm, L. H.; Balk, R. W.; van Koten, G.; Vrieze, K.; Brouwers, A. M. F. *Inorg. Chem.* **1980**, *19*, 3343. (e) Polm, L. H.; van Koten, G.; Elsevier, C. J.; Vrieze, K.; van Santen, B. F. K.; Stam, C. H. *J. Organomet. Chem.* **1986**, *304*, 353.

[7] Keijsper, J.; Polm, L. H.; van Koten, G.; Vrieze, K.; Stam, C. H.; Schagen, J. D. *Inorg. Chim. Acta* **1985**, *103*, 137.

[8] Polm, J. H.; van Koten, G.; Vrieze, K.; Stam, C. H.; van Tunen, W. C. J. *J. Chem. Soc., Chem. Commun.* **1983**, 1177.

[9] (a) Staal, L. H.; van Koten, G.; Vrieze, K.; van Santen, B.; Stam, C. H. *Inorg. Chem.* **1981**, *20*, 3598. (b) Muller, F.; van Koten, G.; Kraakman, M. J. A.; Vrieze, K.; Heijdenrijk, D.; Zoutberg, M. C. *Organometallics* **1989**, *8*, 1331.

[10] (a) Frühauf, H.-W.; Seils, F.; Goddard, R. J.; Romão, M. J. *Angew. Chem.* **1983**, *95*, 1014; *Angew. Chem., Int. Ed. Engl.* **1983**, *22*, 992; *Angew. Chem. Suppl.* **1983**, 1435. (b) Frühauf, H.-W.; Seils, F.; Romão, M. J.; Goddard, R. J. *Organometallics* **1985**, *4*, 948. (c) Frühauf, H.-W.; Seils, F. *J. Organomet. Chem.* **1986**, *302*, 59. (d) Frühauf, H.-W.; Seils, F. *J. Organomet. Chem.* **1987**, *323*, 67. (e) Frühauf, H.-W.; Seils, F.; Stam, C. H. *Organometallics* **1989**, *8*, 2338.

[11] (a) the 1,4-diaza 1,3-dienes of formula R′N=C(R″)C(R″)=NR′ are abbreviated as R′-DAB{R″,R″}. (b) the [2.2.2] bicylic structures are abbreviated as bic.

0276-7333/93/2312-0417$04.00/0

the Fe–N=C unit to give an intermediate [2.2.1] bicyclic structure. This intermediate then readily inserts a carbonyl ligand via a nucleophilic attack of the nitrogen lone pair on the carbonyl carbon atom. The coordinatively and electronically unsaturated [2.2.2] bicyclic structure formed accepts a two-electron-donating additional ligand (L′), leading to an isolable complex. When CO is used as an additional ligand, the resulting bicyclic compound can isomerize via a reductive elimination, followed by recoordination of the double bond, to a 1,5-dihydropyrrol-2-one complex.

To expand the scope of this reaction and to probe the influence of different ligands, we substituted one CO by a CNR ligand in the starting complex $Fe(CO)_3$(R′-DAB). Since cycloaddition reactions are very sensitive to variations in the energetic disposition of the interacting frontier orbitals and since isocyanides are better σ-donating/worse π-accepting[12] ligands than CO, the substitution was expected to lead to an enhanced 1,3-dipolar activity. Also, since isocyanides like CO, are known to undergo insertion reactions, we were interested whether the substitution would lead to a competition between CO and CNR insertion.

In a preliminary publication[1b] we reported that substitution of a CO ligand by *tert*-butyl isocyanide in the starting complex resulted in a reaction in which C–C and C–N coupling of the α-diimine with two molecules of dimethyl acetylenedicarboxylate (DMAD) occurred, leading to the formation of 2,6-diisopropyl-3,4,7,8-tetracarbomethoxy-2,6-diazabicyclo[3.3.0]octa-3,7-diene or tetrahydropyrrolo[3,2-*b*]pyrrole (THPP). In order to investigate in more depth the influence of the ligand substitution, we varied the electronic and steric properties of the isocyanides used. In this paper we now report the results of the reaction of various $Fe(CO)_2$(CNR)(R′-DAB) complexes (1) with DMAD and the single-crystal X-ray structure of 1-isopropyl-2,3-dicarbomethoxy-5-(1,2-dicarbomethoxy-2-(isopropylamino)ethenyl)pyrrole (10).

Already in the 1970s Tolman[13] introduced the approach of cone angles in order to determine the steric properties of phosphines. His results were used in many publications to explain the chemical behavior of different phosphines. Since we used isocyanides in our reactions, we were prompted to estimate their cone angles. The derivation of these cone angles is presented in this publication.

Experimental Section

Solvents were carefully dried and distilled prior to use. All preparations were carried out under an atmosphere of purified nitrogen using Schlenk techniques. All column chromatography was performed using silica gel (Kieselgel 60, 70–230 mesh, E. Merck, Darmstadt, Germany, dried and activated before use) as the stationary phase. Solutions of $Fe(CO)_2$(CNR)(R′-DAB) (1) were prepared according to known procedures.[14] DMAD was used as purchased from Aldrich without purification, CO was obtained from Strem, and $(NH_4)_4Ce(SO_4)_4 \cdot 2H_2O$ was purchased from Merck and used as received. ^1H and ^{13}C NMR spectra were obtained on Bruker AC 100 and AMX 300 spectrometers. IR spectra were recorded with a Perkin-Elmer 283 spectrophotometer (using matched NaCl solution cells). Elemental analyses were carried out by the Elemental Analysis section of the Institute for Applied Chemistry, TNO, Zeist, The Netherlands.

Synthesis of $Fe(CO)_2$(CNR)(R′-THPP) (4) and $Fe(CO)_2$(CNR)([2.2.2]bic)[11b] (7,8). To a solution of $Fe(CO)_2$(CNR)(R′-DAB) (1.60 mmol) in 20 mL of pentane prepared in situ was added a solution of DMAD (3.20 mmol) in 5 mL of Et_2O and 20 mL of pentane at –60 °C over a period of 45 min. The precipitates were washed three times with 20 mL of cold pentane, dried in vacuo, dissolved in 5 mL of Et_2O and 2 mL of CH_2Cl_2, and separated by column chromatography. Elution with Et_2O afforded a yellow fraction which contained $Fe(CO)_2$(CNR)(R′-THPP) (4). Further elution with Et_2O/THF (4/1) yielded a dark yellow fraction which gave, after evaporation of the solvent, $Fe(CO)_2$(CNR)([2.2.2]bic) (7, 8). The total yield of complexes 4, 7, and 8 ranged between 60 and 95%.

Decomplexation of THPP (9). (i) Via Oxidative Decomplexation. A solution of $Fe(CO)_2$(*t*-BuNC)(R′-THPP) (4a; 1.40 mmol) and $(NH_4)_4Ce(SO_4)_4 \cdot 2H_2O$ (4.20 mmol) in 15 mL of benzene was heated to 80 °C. The reaction was monitored by IR spectroscopy and was stopped when the CO and CNR stretching bands had nearly disappeared (approximately 5 days). The solvent was evaporated and the residue purified by column chromatography. Elution with Et_2O afforded a yellow fraction which after evaporation of the solvent yielded the oily THPP (9), yield 60%.

(ii) Via Substitution by CO. A solution of $Fe(CO)_2$(*t*-BuNC)(R′-THPP) (4a; 3.40 mmol) in 50 mL of benzene was placed under 80 bar of CO and heated to 50 °C for a period of 5 days. The solution was evaporated to dryness and separated by column chromatography. Elution with pentane afforded an intense green fraction, containing $Fe_3(CO)_9$(t-BuNC$)_3$ and traces of $Fe(CO)_4$(*t*-BuNC) (identified by IR and ^1H NMR spectroscopy[15]); further elution with Et_2O yielded a yellow fraction which contained the oily THPP (9) in a total yield of 90%.

In order to obtain an analytically pure product, the compound was purified by means of HPLC on a modular Gilson liquid chromatographic system. The columns used were a Dynamax 60-A silica analytical column module (8 μm; 4.8 mm i.d. × 250 mm length in combination with a guard column filled with the same material (50 mm length × 4.8 mm i.d.) and a Dynamax 60-A silica preparative column module, (8 μm; 10.2 mm i.d. × 250 mm length) in combination with a guard column also filled with the same material (50 mm length × 10.2 mm i.d.). The eluent for the separation was a mixture of CH_2Cl_2 and acetonitrile (9/1) and was used isocratically.

Synthesis of the Ethenylpyrrole 10. A solution of THPP (9; 2.1 mmol) in 20 mL of benzene was refluxed for a period of 3 days, dried in vacuo, and purified by column chromatography. Elution with Et_2O resulted in a pale yellow fraction. Evaporation of the solvent yielded the oily ethenylpyrrole 10, yield 95%.

Crystal Structure Determination of the Ethenylpyrrole 10. Crystals were grown from a saturated Et_2O solution at –30 °C. A crystal with approximate dimensions $0.1 \times 0.6 \times 0.35$ mm^3 was used for data collection on an Enraf-Nonius CAD-4 diffractometer with graphite-monochromated Cu Kα radiation and θ–2θ scan. A total of 3765 unique reflections was measured within the range $-9 \leq h \leq 9$, $0 \leq k \leq 34$, $0 \leq l \leq 11$. Of these, 2516 were above the significance level of $2.5\sigma(I)$. The maximum value of (sin θ/λ was 0.59 Å^{-1}. Unit-cell parameters were refined with a least-squares fitting procedure using 23 reflections with 50° ≤

---

[12] (a) Yamamoto, Y.; Yamazaki, H. *Coord. Chem. Rev.* **1972**, *8*, 225. (b) Treichel, P. M. *Adv. Organomet. Chem.* **1973**, *11*, 21. (c) Yamamoto, Y. *Coord. Chem. Rev.* **1980**, *32*, 193.

[13] (a) Tolman, C. A. *J. Am. Chem. Soc.* **1970**, *92*, 2956. (b) Tolman, C. A.; Seidel, W. C.; Gosser, L. W. *J. Am. Chem. Soc.* **1974**, *96*, 53. (c) Tolman, C. A. *Chem. Rev.* **1977**, *77*, 313.

[14] de Lange, P. P. M.; Kraakman, M. J. A.; van Wijnkoop, M.; Frühauf, H.-W.; Vrieze, K.; Smeets, W. J. J.; Spek, A. L. *Inorg. Chim. Acta* **1992**, *196*, 151.

[15] (a) Cotton, F. A.; Parish, R. V. *J. Chem. Soc.* **1960**, 1440. (b) Murray, J. B.; Nicholson, B. K.; Whitton, A. J. *J. Organomet. Chem.* **1990**, *385*, 91.

[16] Walker, N. J.; Stuart, D. *Acta Crystallogr.* **1983**, *A39*, 158.

[17] Stewart, J. M.; Machin, P. A.; Dickinson, C. W.; Ammon, H. L.; Heck, H.; Flack, H. The XRAY76 System; Technical Report TR 446; Computer Science Center, University of Maryland: College Park, MD, 1976.

[18] Cromer, D. T.; Mann, J. B. *Acta Crystallogr.* **1968**, *A24*, 321.

[19] Cromer, D. T.; Mann, J. B. In *International Tables for X-ray Crystallography*; Kynoch Press: Birmingham, U.K., 1974; Vol. IV, p 55.

Table I. Crystal Data and Details of the Structure Determination of Ethenylpyrrole 10

Crystal Data	
formula	$C_{20}H_{28}N_2O_8$
mol wt	424.45
cryst syst	monoclinic
space group	$P2_1/n$
a, b, c (Å)	8.442 (6), 29.240 (7), 9.567 (9)
β (deg)	109.797 (8)
V (Å^3)	2222.5 (4)
Z	4
D_{calc} (g cm^{-3})	1.27
$F(000)$	904
μ (cm^{-1})	7.88 (Cu Kα)
cryst size (mm)	0.1 × 0.6 × 0.35
Data Collection	
temp (K)	293
θ_{min}, θ_{max} (deg)	2.5, 65
radiation	Cu Kα (1.5418 Å)
scan type	$\omega/2\theta$
ref rflns	140, 021
no. of intens measurements	3962
no. of unique rflns	3765
no. of obsd rflns	2516 ($I > 2.5\sigma(I)$)
Refinement	
DIFABS cor range	0.51, 1.19
no. of refined params	384
final R, R_w, S	0.059, 0.083, 0.28
$(\Delta/\sigma)_{max}$ in final cycle	0.28
min and max resd dens (e Å^{-3})	−0.3, 0.3

Table II. Fractional Coordinates of the Non-Hydrogen Atoms and Equivalent Isotropic Thermal Parameters of Ethenylpyrrole 10 (Esd's in Parentheses)

atom	x	y	z	U_{eq} (Å^2)
C1	0.9843 (4)	0.6225 (1)	0.6624 (3)	0.034 (2)
C2	1.0332 (4)	0.6622 (1)	0.7404 (4)	0.037 (2)
C3	0.9179 (4)	0.6717 (1)	0.8143 (3)	0.035 (2)
C4	0.8000 (4)	0.6366 (1)	0.7790 (3)	0.034 (2)
C5	0.7460 (4)	0.5656 (1)	0.6149 (4)	0.042 (2)
C6	0.5890 (5)	0.5786 (2)	0.4868 (5)	0.066 (3)
C7	0.7105 (6)	0.5341 (1)	0.7259 (5)	0.063 (3)
C8	0.6470 (4)	0.6333 (1)	0.8226 (4)	0.044 (2)
C9	0.5406 (6)	0.6155 (2)	1.0120 (5)	0.080 (3)
C10	0.9152 (4)	0.7096 (1)	0.9124 (4)	0.039 (2)
C11	1.0497 (6)	0.7779 (2)	1.0245 (5)	0.071 (3)
C12	1.0601 (4)	0.5986 (1)	0.5648 (4)	0.035 (2)
C13	1.0469 (4)	0.6177 (1)	0.4292 (4)	0.038 (2)
C14	1.1080 (5)	0.6213 (1)	0.1903 (4)	0.051 (2)
C15	1.1168 (6)	0.5823 (2)	0.0886 (4)	0.068 (3)
C16	1.2469 (5)	0.6559 (2)	0.2070 (5)	0.065 (3)
C17	1.1536 (4)	0.5563 (1)	0.6106 (4)	0.041 (2)
C18	1.2392 (6)	0.4991 (2)	0.7946 (6)	0.075 (3)
C19	0.9353 (4)	0.6595 (1)	0.3819 (4)	0.042 (2)
C20	0.9250 (7)	0.7398 (2)	0.3669 (7)	0.080 (3)
N1	0.8403 (3)	0.60698 (9)	0.6865 (3)	0.034 (1)
N2	1.1191 (4)	0.6017 (1)	0.3350 (3)	0.050 (2)
O1	0.5091 (3)	0.6447 (1)	0.7448 (3)	0.075 (2)
O2	0.6796 (3)	0.6161 (1)	0.9569 (3)	0.058 (2)
O3	0.8157 (4)	0.7139 (1)	0.9763 (4)	0.069 (2)
O4	1.0383 (3)	0.73951 (9)	0.9238 (3)	0.056 (2)
O5	1.2215 (3)	0.53471 (3)	0.5386 (3)	0.056 (2)
O6	1.1571 (3)	0.54248 (9)	0.7466 (3)	0.053 (1)
O7	0.7862 (3)	0.6569 (1)	0.3316 (3)	0.062 (2)
O8	1.0230 (3)	0.69747 (9)	0.4044 (3)	0.060 (2)

$2\theta \le 58°$. Corrections for Lorentz and polarization effects were applied. The non-hydrogen atoms were found by direct methods using SIMPEL.[20] The hydrogen atoms were calculated on the basis of standard geometry. Block-diagonal least-squares refinement on F, anisotropic for the non-hydrogen atoms and isotropic for the hydrogen atoms, which were retained in such a way that the distance to their carrier atoms was kept fixed at 1.09 Å, converged to $R = 0.059$, $R_w = 0.083$, and $(\Delta/\sigma)_{max} = 0.28$. The weighting scheme $w = (3.56 + F_o + 0.0146F_o^2)^{-1}$ was used. A final difference Fourier map revealed a residual electron density between −0.3 and +0.3 e Å^{-3}. Scattering factors were taken from Cromer and Mann.[18] All calculations were performed with XTAL3.0[21] unless stated otherwise. Crystal data and numerical details of the structure determination are given in Table I. Final atomic coordinates and equivalent isotropic thermal parameters of the non-hydrogen atoms are given in Table II.

Results

The ligands and complexes employed are shown in Scheme I. The type of complex is identified by arabic numbers. The different isocyanides are differentiated by the letters **a–f**. All complexes bear *i*-Pr groups on the DAB nitrogen atoms, except for the complexes identified by the letter **g**, which contain a c-Hex group on the DAB nitrogen atoms.

$Fe(CO)_2(CNR)(R'\text{-DAB})$ (**1**) reacts with the electron-deficient DMAD to give three products. One product results from the reaction of two alkyne molecules with both imine units, leading to $Fe(CO)_2(CNR)(R'\text{-THPP})$ (**4**). The other two are [2.2.2] bicyclic structures with either an inserted CNR ligand (**7**) or an inserted CO ligand (**8**). The product distribution (see Table III) depends on the isocyanide used. Only in the case of the aromatic isocyanides **e** and **f** are [2.2.2] bicyclic complexes with inserted isocyanides formed, whereas with the aliphatic isocyanides **a–d** no isocyanide insertion has been observed.

The molecular structure of $Fe(CO)_2(t\text{-BuNC})(i\text{-Pr-THPP})$ (**4a**) consists of a $Fe(CO)_2(t\text{-BuNC})$ unit η^3-bonded through a N atom and the double bond of one of the two pyrrole rings. This molecular structure was confirmed by an X-ray single-crystal structure determination and reported previously.[1b]

The heterocycle **9**, synthetically interesting due to the presence of two enamine units,[22] can be decomplexed by placing the organometallic complex **4** under 80 bar of CO pressure. This results in the formation of free THPP (**9**) and of the intense green trimer $Fe_3(CO)_9(CNR)_3$,[15b] as a consequence of recombination of $Fe(CO)_2(CNR)$ fragments and CO molecules. The heterocycle can also be displaced from the metal by treatment of the transition-metal compound with a Ce(IV) salt. This method suffers from the drawback that for prolonged reaction times the decomplexed THPP **9** isomerizes to the ethenylpyrrole **10**. Ethenylpyrrole **10** has also been formed by starting from free THPP in refluxing benzene via a bond fission which opens one of the pyrrole rings, leading to the

---

(20) Schenk, H.; Hall, S. R. In *SIMPEL XTAL3.0 Reference Manual*; Hall, S. R., Stewart, J. M., Eds.; Universities of Western Australia and Maryland, Nedlands, WA, and College Park, MD, 1990.

(21) Hall, S. R., Stewart, J. M., Eds. *XTAL3.0 Reference Manual*; Universities of Western Australia and Maryland, Nedlands, WA, and College Park, MD, 1990.

(22) (a) Satake, K.; Kumagai, T.; Mukai, T. *Chem. Lett.* **1983**, 743. (b) Kumagai, T.; Tanaka, S.; Mukai, T. *Tetrahedron Lett.* **1984**, *25*, 5669. (c) Satake, K.; Kumagai, T.; Mukai, T. *Chem. Lett.* **1984**, 2036. (d) Mukai, T.; Konno, A.; Kumagai, T.; Satake, K. *Chem. Lett.* **1985**, 1809.

(23) Ayyangar, N. R.; Bambal, R. B.; Srinivasan, K. V.; Guru Row, T. N.; Puranik, V. G.; Tavale, S. S.; Kulkarni, P. S. *Can. J. Chem.* **1986**, 1969.

(24) (a) Merola, J. S.; Kacmarcik, R. T.; van Engen, D. *J. Am. Chem. Soc.* **1986**, *108*, 329. (b) Kowaleski, R. M.; Rheingold, A. L.; Trogler, W. C.; Basolo, F. *J. Am. Chem. Soc.* **1986**, *108*, 2460. (c) Nesmeyanov, A. N.; Ustynyuk, N. A.; Makarova, L. G.; Andrianov, V. G.; Struchkov, Y. T.; Andrea, S.; Ustynyuk, Y. A.; Malyugina, S. G. *J. Organomet. Chem.* **1978**, *159*, 189.

(25) (a) Singleton, E.; Oosthuizen, H. E. *Adv. Organomet. Chem.* **1983**, *22*, 209. (b) Bonati, F.; Minghetti, G. *Inorg. Chim. Acta* **1974**, *9*, 95. (c) Carmona, E.; Galindo, E.; Matin, J. M. *Polyhedron* **1988**, *7*, 1831. (d) Bassett, J. N.; Berry, D. E.; Barker, G. K.; Green, M.; Howard, J. A. K.; Stone, F. G. A. *J. Chem. Soc., Dalton Trans.* **1979**, 1003.

Scheme I. Reactions of $Fe(CO)_2(CNR)(DAB)$ with DMAD

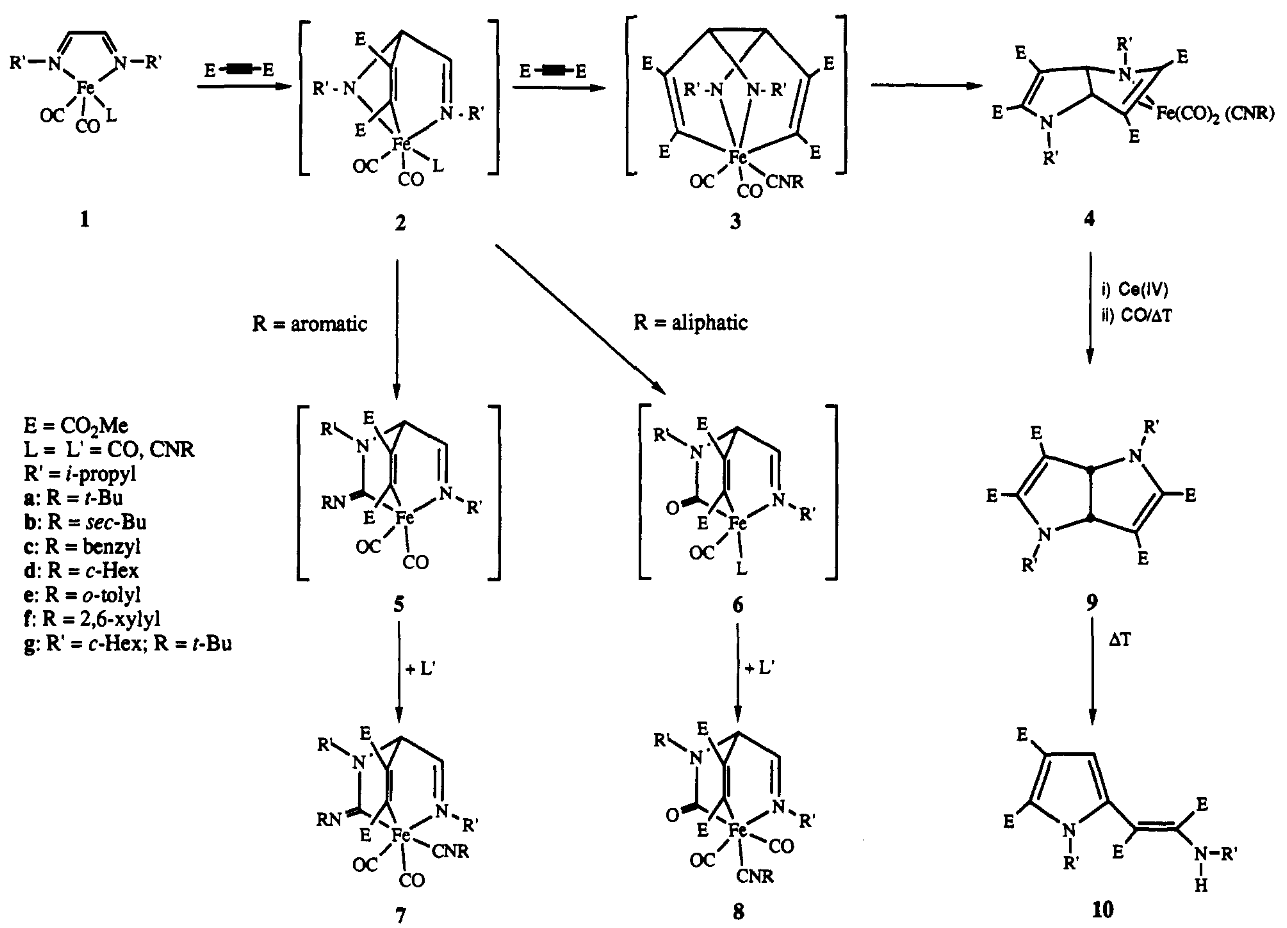

Table III. Product Distribution (%) of $Fe(CO)_2(CNR)(R'\text{-THPP})$ (4) and $Fe(CO)_2(CNR)([2.2.2]bic)$ (7 and 8) Using Various CNR Groups

CNR	THPP (4)	bicyclo[2.2.2] (7)	bicyclo[2.2.2] (8)
t-Bu (a)	>95		<5
sec-Bu (b)	80		20
benzyl (c)	80		20
c-Hex (d)	70		30
o-tolyl (e)	10	90	
2,6-xylyl (f)	20	80	

formation of an enamine. The molecular structure of the ethenylpyrrole will be described below.

In Scheme I the two imine units in the starting α-diimine ligand are first transformed into amines in THPP 9 and secondly one of the C–N bonds is broken, resulting in ethenylpyrrole 10.

Molecular Structure of the Ethenylpyrrole 10. The molecular structure of the organic compound 10 together with the atomic numbering is shown in Figure 1. In Tables IV and V bond distances and bond angles are summarized.

The bond distances within the pyrrole ring vary from 1.361 (4) to 1.411 (5) Å, indicating a delocalization of the nitrogen lone pair and the two double bonds, which is normal for 1*H*-pyrrole.[26] Very interesting are the bond lengths and bond angles in the enamine unit. The formal double bond C12–C13 has been slightly elongated to 1.318 (5) Å, while the C13–N2 formal single bond has been shortened to 1.333 (5) Å. (Normal bond lengths found for a C–C double and a C–N single bond are 1.34 and 1.40 Å, respectively.[26]) The bond angles around C12, C13, and N2 are all 120°, which is in agreement with an sp^2 hybridization. All this can be explained by a conjugation of the nitrogen lone pair and the double bond (see Scheme II). These resonance structures have also been encountered in the analogous enamine carbaldehydes.[27] The negative charge on C12 in the resonance structures is probably stabilized via conjugation with the ester function. The fact that the two delocalized systems cannot couple to one totally delocalized structure is reflected by the C1–C12 bond lengths of 1.475 (5) Å, showing no double-bond character, and can also be deduced from the angle of 106.3° between the plane of C12–C13–N2 and the planar pyrrole ring.

NMR Spectroscopy. ^1H NMR and ^{13}C NMR data for $Fe(CO)_2(CNR)(bic)$ (7, 8), $Fe(CO)_2(CNR)(R'\text{-THPP})$ (4), *i*-Pr-THPP 9, and ethenylpyrrole 10 are listed in Tables VI and VII.

^1H NMR. The signals for the inserted isocyanides of complexes 7 and 8 are interesting. Upon insertion, the isocyanides have lost a rotational degree of freedom. This results in an inequivalency of the aromatic substituents. Therefore, in the case of the 2,6-xylyl isocyanide, the two methyl groups resonate at 2.44 and 2.55 ppm. The two meta protons give rise to a set of two doublets from which, due to the bulk of the aromatic signals, only one doublet at 6.93 ppm (J = 7 Hz) is visible; the para proton gives a double doublet at 6.78 ppm. Due to the equivalent coupling constants (J = 7 Hz) the signal appears as a triplet.

---

(26) Allen, F. H.; Kennard, O.; Waton, D. G.; Brammer, L.; Orpen, A. G.; Taylor, R. *J. Chem. Soc., Perkin Trans. 2* **1987**, S1.

(27) Tietze, L. F.; Bergmann, A.; Brill, G.; Brüggemann, K.; Hartfiel, U.; Voss, E. *Chem. Ber.* **1989**, *122*, 83.

(28) Kozerski, L. *Tetrahedron* **1976**, *32*, 1299.

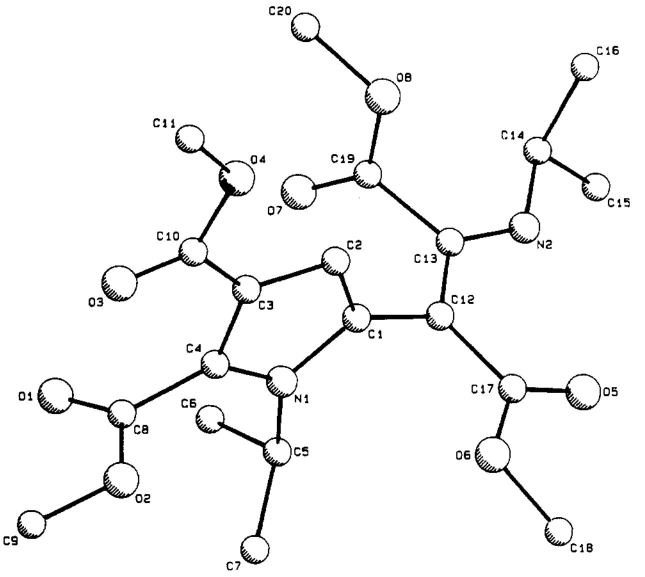

Figure 1. PLUTO drawing of 1-isopropyl-2,3-dicarbomethoxy-5-(1,2-dicarbomethoxy-2-(isopropylamino)ethenyl)pyrrole (10).

Table IV. Bond Lengths (Å) for the Non-Hydrogen Atoms of Ethenylpyrrole 10 (Esd's in Parentheses)

C1–C2	1.366 (4)	C1–C12	1.475 (5)	C1–N1	1.388 (5)
C2–C3	1.411 (5)	C3–C4	1.388 (4)	C3–C10	1.459 (5)
C4–C8	1.489 (6)	C4–N1	1.361 (4)	C5–C6	1.518 (5)
C5–C7	1.511 (6)	C5–N1	1.482 (4)	C8–O1	1.197 (4)
C8–O2	1.318 (5)	C9–O2	1.411 (6)	C10–C3	1.201 (6)
C10–O4	1.334 (4)	C11–O4	1.461 (5)	C12–C13	1.381 (5)
C12–C17	1.453 (5)	C13–C19	1.516 (5)	C13–N2	1.333 (5)
C14–C15	1.518 (6)	C14–C16	1.516 (6)	C14–N2	1.472 (5)
C17–O5	1.211 (5)	C17–O6	1.353 (5)	C18–O6	1.443 (5)
C19–O7	1.188 (4)	C19–O8	1.311 (4)	C20–O8	1.463 (5)

A similar effect is visible for the *o*-tolyl isocyanide. Although *o*-tolyl isocyanide is unsymmetrically substituted to begin with, after insertion, instead of a multiplet, a set of doublets and double doublets shifted to high field is visible.

Asymmetric coordination of the THPP ligand in 4 results in two doublets for the former imine protons at the bridgehead positions and in four singlets for the ester methoxy groups. When the $Fe(CO)_2(CNR)$ fragment is removed, the free pyrrolopyrrole 9 obtains C_2 symmetry with the C_2 axis perpendicular to the central C–C bond. Consequently, the two bridgehead protons appear in the ^1H NMR spectrum as a singlet and the four methoxy groups give rise to only two singlets.

Upon ring opening of the pyrrolopyrrole 9 four inequivalent methyl groups of the ester units are regenerated in 10. The proton on the pyrrole ring resonates at 6.24 ppm, a value commonly found for pyrrole protons.[29] The proton which is localized on the nitrogen atom gives a doublet (J = 7 Hz) at 3.91 ppm. The methyne proton of the isopropyl group is split into a double septet, at 3.40 ppm, due to coupling with the two methyl groups and with the nitrogen proton. This coupling unequivocally indicates that the hydrogen is located at the nitrogen.

^{13}C NMR. The characteristic features of the [2.2.2] bicyclic structures 7 and 8 are clearly visible in the ^{13}C NMR spectra (see Table VII).

The asymmetry of the complex $Fe(CO)_2(CNR)$(R'-THPP) (4) can also be deduced from the ^{13}C NMR spectrum.[30] The four different carboxy carbon atoms resonate at four different frequencies. The carboxy carbon atoms on the uncoordinated pyrrole ring resonate at about 168 and 164 ppm, while those on the coordinated pyrrole ring resonate near 176 and 217 ppm. The last value is remarkable. This low-field shift of one of the carboxy carbon atoms can only be explained by an interaction of one of the ester carbonyl groups with the metal.[31] The coordination of the carbonyl oxygen of an ester group has been encountered before. Torres et al.[32] have described the molecular structure of a ruthenium compound in which an ester carbonyl of a former alkyne is coordinated to the metal. A comparatively large shift (ca. 50 ppm) of a carboxy function has also been reported by Johnson et al.[34] for a ruthenium A-frame complex in which an acyl carboxy carbon atom is shifted from 247.8 to 293.8 ppm upon coordination of the oxygen to the metal. Also, Guilbert et al.[35] have published a value of 225 ppm for an acyl carbon atom coordinated via oxygen. However, in the solid state the coordination of an ester carbonyl in 4 is not supported by the results of the X-ray analysis.[1b] The iron–carbonyl oxygen distances were found to be 4.190 (4) and 3.625 (5) Å. Although one of the ester carbonyls is closer to the iron atom, the distances are too large to confirm coordination. At 293 K the ^{13}C resonances of the two CO ligands appear as one singlet at 214 ppm, which points to a scrambling of the CO's, and as expected, upon cooling to 243 K the signal is split into two signals.

The organometallic $Fe(CO)_2(CNR)$(R'-THPP) complex (4) shows an intriguing behavior in solution: depending on the temperature two sets of signals are visible. This can be rationalized by a temperature-dependent equilibrium of either conformational or coordinational isomers, which at elevated temperature is completely shifted to one side. Although the possibility of conformational isomers cannot be rigorously excluded, we prefer to explain the observations by two coordinational isomers, which are both N,π-coordinated (cf. Figure 2 and the following discussion). The behavior is best illustrated by the resonances of the alkene carbon atoms and the bridgehead carbon atoms of $Fe(CO)_2$(*t*-BuNC)(*i*-Pr-THPP) (**4a**). At high temperature (323 K) the bridgehead carbon atoms resonate at 72.1 and 67.2 ppm (cf. B in Figure 2). The coordinated alkene carbon atoms give rise to signals at 55.5 and 85.7 ppm; the alkene carbon atoms of the uncoordinated pyrrole ring resonate at 94.2 and 165.9 ppm. These coordination shifts of ca. 37 and 78 ppm to low field are in the normal range found for π-coordinated alkenes.[36]

---

[29] Hesse, M.; Meier, H.; Zeeh, B. In Spektroskopische Methoden in der Organischen Chemie; Georg Thieme Verlag: Stuttgart, Germany, and New York, 1984.

[30] Some of the values reported before[1b] have been corrected.

[31] Unfortunately, it is not possible to confirm the interaction by IR spectroscopy. Coordination should result in a shift to lower wavenumber (ca. 1600 cm^{-1})[32,33] for the frequency of the ester group, compared to the frequency of an uncoordinated ester function. However, due to the presence of other bands in the same region the appearance of such a band is obscured.

[32] Torres, M. R.; Santos, A.; Ros, J.; Solans, X. *Organometallics* **1987**, *6*, 1091.

[33] (a) Blackmore, T.; Bruce, M. I.; Stone, F. G. A. *J. Chem. Soc., Dalton Trans.* **1974**, 106. (b) Grevels, F.-W.; Reuvers, J. G. A.; Takats, J. *Angew. Chem.* **1981**, *93*, 475. (c) Foulger, B. E.; Grevels, F.-W.; Hess, D.; von Gustorf, E. A. K.; Leitich, J. *J. Chem. Soc., Dalton Trans.* **1979**, 1451. (d) Rouston, J. L.; Charrier, C.; Mérour, J. Y.; Bénaïm, J. *J. Organomet. Chem.* **1973**, *38*, C37. (e) Bruce, M. I.; Gardner, R. C. F.; Stone, F. G. A. *J. Chem. Soc., Dalton Trans.* **1979**, 906.

[34] Johnson, A. K.; Gladfelter, W. L. *Organometallics* **1990**, *9*, 2101.

[35] Guilbert, B.; Demerseman, B.; Dixneuf, P. H.; Mealli, C. *J. Chem. Soc., Chem. Commun.* **1989**, 1035.

[36] Mann, B. E. *Adv. Organomet. Chem.* **1974**, *12*, 135.

Table V. Bond Angles (deg) for the Non-Hydrogen Atoms of Ethenylpyrrole 10 (Esd's in Parentheses)

C2–C1–C12	129.3 (3)	C2–C1–N1	107.9 (3)	C12–C1–N1	122.9 (3)
C1–C2–C3	108.0 (3)	C2–C3–C4	107.0 (3)	C2–C3–C10	129.5 (3)
C4–C3–C10	123.5 (3)	C3–C4–C8	126.8 (3)	C3–C4–N1	108.2 (3)
C8–C4–N1	124.8 (3)	C6–C5–C7	113.2 (3)	C6–C5–N1	110.7 (3)
C7–C5–N1	112.1 (3)	C4–C8–O1	124.1 (4)	C4–C8–O2	112.5 (3)
O1–C8–O2	123.4 (4)	C3–C10–O3	124.9 (3)	C3–C10–O4	111.7 (3)
O3–C10–O4	123.4 (3)	C1–C12–C13	119.2 (3)	C1–C12–C17	121.4 (3)
C13–C12–C17	119.4 (3)	C12–C13–C19	116.8 (3)	C12–C13–N2	125.7 (3)
C1–C13–N2	117.5 (3)	C15–C14–C16	111.5 (4)	C15–C14–N2	108.0 (3)
C16–C14–N2	111.1 (3)	C12–C17–O5	125.8 (3)	C12–C17–O6	112.1 (3)
O5–C17–O6	122.1 (3)	C13–C19–O7	122.3 (3)	C13–C19–O8	112.0 (3)
O7–C19–O8	125.7 (3)	C1–N1–C4	109.0 (3)	C1–N1–C5	123.6 (3)
C4–N1–C5	127.4 (3)	C13–N2–C14	127.0 (3)	C8–O2–C9	115.7 (3)
C10–O4–C11	115.6 (4)	C17–O6–C18	114.8 (3)	C19–O8–C20	115.8 (3)

Scheme II. Resonance Structures of Ethenylpyrrole 10

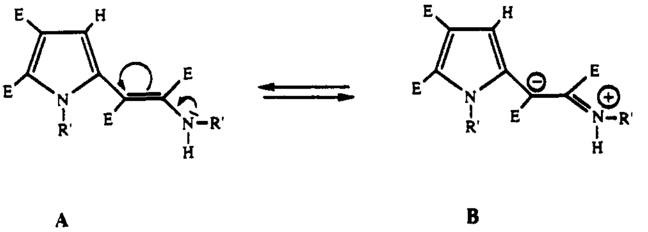

When the solution of complex **4a** is cooled, another set of signals close to the first one becomes visible, and at 243 K, the two sets are of about equal intensity. The bridgehead carbon atoms now also give rise to signals at 71.0 and 66.6 ppm (cf. A in Figure 2). The alkene carbon atoms of the π-coordinated double bond resonate at 53.2 and 84.7 ppm, while the uncoordinated alkene carbon atoms give rise to signals at 93.8 and 158.4 ppm.

An assignment of structure A to the low-temperature isomer is based on the assumption that this structure, which is also found in the crystal, should be of lower energy. At 323 K only situation B is valid. Upon cooling, isomer A also becomes visible. As a consequence of coordination to the metal, the nitrogen lone pair is not available for delocalization with the double bond. The effect of a coordinated or noncoordinated nitrogen atom should most strongly influence the shift of the β-carbon atoms. However, as was already deduced from single-crystal X-ray crystallography[1b] there is only a small amount of delocalization in the N—C=C fragment. Consequently, the influence of the coordinated or noncoordinated nitrogen atom is mainly inductive, and the shifts of the β-carbon atoms in structures A and B are comparable. This temperature-dependent structural behavior in solution shows marked differences to that of $Ru(CO)_3$(*i*-Pr-THPP), which we have also investigated.[1a] Whereas here the iron is always coordinated to one of the π-acidic double bonds, the ruthenium not only forms a coordination isomer with N,N′-coordinated THPP but also becomes fluxional, and the $Ru(CO)_3$ moiety starts moving around the perimeters of both rings before the complex falls apart, liberating THPP.

Just as in the ^{1}H NMR spectrum (vide supra), the ^{13}C NMR spectrum of **9** reflects the high degree of symmetry of *i*-Pr-THPP. The four methoxy carbon atoms resonate at 165.0 and 164.4 ppm. The alkene carbon atoms now give rise to only two signals at 155.8 and 95.7 ppm, from which it becomes clear that all four alkene carbon atoms are sp^2-hybridized. Comparable values have also been encountered in one set of the alkene carbon atoms in complex **4**, which shows that the $Fe(CO)_2(CNR)$ moiety in neither of the coordination isomers is bonded to more than one C–C double bond.

The asymmetry of compound **10** is clearly visible in the ^{13}C NMR spectrum. The four methoxy carbon atoms of the ester groups give rise to four signals. The four pyrrole carbon atoms resonate at 111.1, 115.2, 127.3, and 128.9 ppm, which is in the common range for pyrrole compounds.[29] The frequencies of the two alkene carbon atoms show the influence of the resonance structures discussed in the molecular structure (see Scheme II). C13 (see Figure 1 for atomic numbering) resonates at 156.0 ppm, while C12 resonates at 83.5 ppm. This high-field shift is a result of the negative charge which resides on C12 according to resonance structure B.

IR Spectroscopy. The IR data of the [2.2.2] bicyclic complexes **7** and **8**, the $Fe(CO)_2(CNR)(R'\text{-THPP})$ complexes **4**, THPP **9**, and ethenylpyrrole **10** are collected in Table VIII, together with the elemental analyses. The IR spectra of the bicyclic and the $Fe(CO)_2(CNR)(R'\text{-THPP})$ complexes show one CNR and two intense CO stretching vibrations. The shift of ca. 20 cm^{-1} to lower frequency of the isocyanide stretching vibration of the bicyclic complexes with an aromatic isocyanide, compared to those with an aliphatic isocyanide ligand, is a result of the better electron-withdrawing capacities of the phenyl group,[14,37] which reduces the C≡N bond order. The CO stretching vibrations of the $Fe(CO)_2(CNR)(R'\text{-THPP})$ complexes **4** have shifted ca. 30–50 cm^{-1} to lower frequency with respect to those of the [2.2.2] bicyclic complexes **7** and **8**. The shift to lower frequency is a logical consequence of going from an Fe(II) to a Fe(0) complex. For the isocyanide stretching vibrations the same trend is observed as in the bicyclic compounds.

The IR spectrum of the ethenylpyrrole compound **10** confirms the presence of the enamine form by a broad N–H absorption at 3400 cm^{-1}.

Discussion

Cone Angle Measurements for Isocyanide Ligands. In order to gauge the steric influences of the isocyanide ligands on the course of the cycloaddition reaction, we have determined isocyanide cone angles. We have used an approach and a ligand angle measuring device similar to the one Tolman has employed to determine the angles for phosphines[13] and Trogler et al. for amine ligands.[38]

---

[37] (a) Saillard, J. Y.; Le Beuze, A.; Simmoneaux, G.; Le Maux, P.; Jaouen, G. *J. Mol. Struct.* **1981**, *86*, 149. (b) Minelli, M.; Maley, W. J. *Inorg. Chem.* **1989**, *28*, 2954. (c) Fantucci, P.; Naldini, L.; Cariati, F.; Valenti, V.; Bussetto, C. *J. Organomet. Chem.* **1974**, *64*, 109. (d) Malatesta, L.; Bonati, F. In *Isocyanide Complexes of Metals*; Wiley: New York, 1969; p 7.

[38] Seligson, A. L.; Trogler, W. C. *J. Am. Chem. Soc.* **1991**, *113*, 2520.

Table VI. ^{1}H NMR Data[a] for Fe(CO)$_2$(CNR)(R′-THPP) (4), Fe(CO)$_2$(CNR)([2.2.2]bic) (7, 8), *i*-Pr-THPP (9), and Ethenylpyrrole (10)

compd	^{1}H NMR data[b]
4a	4.90, 4.56 (2 × 1H, d, 9 Hz, bridgehead H), 3.84, 3.77, 3.59, 3.54 (4 × 3 H; 4 × s; OCH_3; 2H, m, CH(CH$_3$)$_2$), 1.43 (9 H, s, N≡CC(CH_3)$_3$), 1.33, 1.28, 1.20, 1.02 (4 × 3 H, 4 × d, 7 Hz, CH(CH_3)$_2$
4b	4.96, 4.48 (2 × 1 H, d, 9 Hz, bridgehead H), 3.87, 3.79, 3.63, 3.59 (4 × 3H, 4 × s; OCH_3; 2H, m, CH(CH$_3$)$_2$), 1.06–1.37 (21H, m, CH(CH_3)$_2$, *sec*-BuH)
4c	7.39 (5H, m, aryl H), 4.97, 4.48 (2 × 1 H, d, 9 Hz, bridgehead H), 4.93 (2H, m, CH_2 aryl) 3.87, 3.81, 3.70, 3.63 (4 × 3H, 4 × s; OCH_3; 2H, m, CH(CH$_3$)$_2$), 1.27–1.58 (12H, m, CH(CH_3)$_2$)
4d	4.96, 4.48 (2 × 1H, d, 9 Hz; bridgehead H), 3.89, 3.81, 3.64, 3.60 (4 × 3H, 4 × s; OCH_3; 2H, m, CH(CH$_3$)$_2$; 1H, m, c-Hex CH), 1.00–1.92 (22H, m, CH(CH_3)$_2$, c-Hex CH_2)
4f	7.10 (3H, m, aryl H), 5.02, 4.56 (2 × 1H, d, 9 Hz, bridgehead H), 3.89, 3.83, 3.78, 3.76 (4 × 3H, 4 × s; OCH_3; 2H, m, CH(CH$_3$)$_2$) 2.43 (6H, s, aryl CH_3), 1.42, 1.35, 1.31,1.15 (4 × 3H, 4 × d, 7 Hz, CH(CH_3)$_2$)
4g	4.96, 4.43 (2 × 1H, d, 9 Hz; bridgehead H), 3.88, 3.78, 3.64, 3.59 (4 × 3H, 4 × s; OCH_3), 3.43 (1H, m, c-Hex CH), 1.70–1.12 (10H, m; c-Hex CH_2), 1.42 (9H, s, N≡CC(CH_3)$_3$)
7e	8.51 (1H, d, 5 Hz, HC=N), 7.41–7.11 (5H, m, aryl H), 7.05, 6.73 (2 × 1H, 2 × d, 7 Hz; *o* aryl H, *m* aryl H), 6.85 (1H, dd, 7 Hz, 7 Hz, *m* or *p* aryl H), 5.89 (1H, d, 5 Hz, N=CCH), 5.03, 4.04 (2 × 1H, 2 × sept, 7 Hz, CH(CH$_3$)$_2$), 3.73, 3.79 (2 × 3H, 2 × s, OCH_3), 2.39, 2.09 (2 × 3H, 2 × s, aryl CH_3), 1.39, 1.23, 1.21, 1.15 (4 × 3H, 4 × d, 7 Hz; CH(CH_3)$_2$)
7f	8.44 (1 H, d, 5 Hz; HC=N), 7.28–6.95 (4 H, m, aryl H), 6.93 (1H, d, 7 Hz; *m* aryl H), 6.78 (1H, dd, 7 Hz, 7 Hz, *p* aryl H), 5.84 (1H, d, 5 Hz; N=CCH), 4.80, 4.06 (2 × 1H, 2 × sept, 7 Hz; CH(CH$_3$)$_2$), 3.67, 3.59 (2 × 3H, 2 × s, OCH_3), 2.55, 2.44 (2 × 3H, 2 × s; C=N aryl CH_3), 2.18 (6H, s, C≡N aryl CH_3), 0.83–1.38 (12H, m, CH(CH_3)$_2$)
8a	8.35 (1H, d, 5 Hz, HC=N), 5.72 (1H, d, 5 Hz, N=CCH), 3.83, 4.68 (2 × 1H, 2 × sept, 6 Hz, CH(CH$_3$)$_2$), 3.73, 3.60 (2 × 3H, 2 × s, OCH_3), 1.44 (9H, s, C(CH_3)$_3$), 0.9–1.38 (12H, m, CH(CH_3)$_2$)
8b	8.35 (1H, d, 5 Hz, HC=N), 5.73, (1H, d, 5 Hz, N=CCH), 4.79, 3.86 (2 × 1H, 2 × sept, 6 Hz, CH(CH$_3$)$_2$), 3.74, 3.79 (2 × 1H, 2 × s, OCH_3), 1.66 (1H, m, NC(H)(C)CC), 0.97–1.42 (20H, m, CH(CH_3)$_2$, *sec*-Bu H)
8c	8.35 (1H, d, 5 Hz; HC=N), 7.34 (5H, m, aryl H), 5.76 (1H, d, 5 Hz, N=CCH), 4.84 (3H, m, CH(CH$_3$)$_2$, CH_2 aryl), 3.88 (1H, sept, 6 Hz, CH(CH$_3$)$_2$), 3.71, 3.51 (2 × 1H, 2 × s, OCH_3), 1.27, 1.18, 1.05, 0.98 (4 × 3H, 4 × d, 6 Hz; CH(CH_3)$_2$)
8d	8.35 (1H, d, 5 Hz, HC=N), 5.73 (1H, d, 5 Hz, N=CCH), 4.82, 3.92 (2 × 1H, 2 × sept, 7 Hz, CH(CH$_3$)$_2$), 3.78, 3.79 (2 × 3H, 2 × s, OCH_3; 1H, m, c-Hex CH), 0.91–1.43 (23H, m, CH(CH_3)$_2$, c-Hex CH_2)
9	5.34 (2H, s, bridgehead H), 3.91, 3.67 (2 × 3H, 2 × s, OCH_3), 3.86 (2H, sept, 7 Hz, CH(CH$_3$)$_2$), 1.30, 1.26, 1.25, 1.24 (4 × 3H, d, 7 Hz, CH(CH_3)$_2$)
10	9.81 (1H, d, 9 Hz, NH), 6.24 (1H, s, pyrrole H), 4.31 (1H, sept, 7 Hz, pyrrole CH(CH$_3$)$_2$), 3.91, 3.75, 3.63, 3.55 (4 × 3H, 4 × s, OCH_3), 3.43 (1H, d sept, 7 Hz, 9 Hz, N(H)CH(CH$_3$)$_2$), 1.43, 1.39, 1.29, 1.23 (4 × 3H, 4 × d, 7 Hz, CH(CH_3)$_2$)

[a] The chemical shift values, in ppm relative to Me$_4$Si, were measured in CDCl$_3$ at 298 K and 300.15 MHz. [b] Abbreviations: s = singlet, d = doublet, m = multiplet.

This device consists of a block to which a side arm is connected. Into a hole in the geometric center of the block is placed a supporting pin, machined to accept Ealing connectors. CPK atomic models from the Ealing Corp., Cambridge, MA, are used to make models of the various isocyanide ligands. With this device, cone angles measured for several phosphine ligands are within 3° of those reported by Tolman. An average metal–terminal isocyanide carbon atom (*C*NR) distance of 1.99 Å[39] is taken for the cone angles reported in Table IX. This value was determined after a search in the Cambridge Structural Data base System[40] for all recorded X-ray structures of transition-metal isocyanide complexes. (The distances varied between 1.70 and 2.32 Å).

For the determination of isocyanide cone angles (θ) some suppositions had to be made. First, the M—C≡N—C arrangement is said to be linear. Second, the substituents are folded in such a way as to minimize the cone angle, analogous to the Tolman approach. This folding is not without problems because of the many internal degrees of freedom present.[41,42] Figure 3 indicates how an effective cone angle can be defined for an unsymmetrical ligand, C≡N—C(R$_1$R$_2$R$_3$), by using a model to minimize the sum of the half-angles given in Tolman's[13] equation (eq 1). In

$$\theta = {}^2/_3\sum_{i=1}^{3}\theta_i/2 \tag{1}$$

the case of aromatic isocyanides we adapted eq 1. The resulting equation (2) takes into account the four sides of a phenyl ring.

$$\theta = {}^2/_4\sum_{i=1}^{4}\theta_i/2 \tag{2}$$

For the determination of the isocyanide cone angles two approaches were applied. The first one (hereafter named the *remote cone angle approach*) is analogous to the one Tolman has used, by setting the van der Waals radius of the isocyano group (C≡N) to zero. When this is done, only the effects of the substituents are considered. In the second approach, henceforth called the *nearby cone angle approach*, the van der Waals radius of the isocyano carbon atom (*C*≡N) is fully taken into consideration. The difference between the two approaches becomes important for ligands with small substituents. For the cone angle of phosphines DeSanto et al.[41] stated that by incorporating the van der Waals radius of the central phosphorus atom, with an arbitrary van der Waals radius of 1.6 Å for phosphorus, the half-angle would always have a minimum value of 44.6°. Since the half-angle of P–H is smaller, this minimum value would hide the P–H hydrogen influence on the phosphorus cone angle. Consequently, all phosphorus cone angles of phosphorus ligands with hydrogen substituents should be incorrect. Because the nearby cone angle approach takes the complete ligand into account, we intuitively prefer the nearby cone angle approach over that of the remote cone angle. The specific difference between the two approaches can be visualized by two more or less extreme situations. It can be depicted that the remote cone angle is especially important for those cases where a substrate approaches a complex. An incoming substrate will first experience steric influences of a coordinated isocyanide by the remote cone angle. The

---

[39] The mean metal–CNR distance proved to be independent of the character of the R group (i.e. aliphatic vs aromatic).

[40] Cambridge Structural Data Base System version 3.4 user's manual part I (Quest 89) and part II (GSTAT89 & PLUTO89), July 1991 release, included 90 296 entries.

[41] DeSanto, J. T.; Mosbo, J. A.; Storhoff, B. N.; Bock, P. L.; Bloss, R. E. *Inorg. Chem.* 1980, *19*, 3086.

[42] Alyea, E. C.; Dias, S. A.; Ferguson, G.; Restivo, R. J. *Inorg. Chem.* 1977, *16*, 2329.

Table VII. ^{13}C NMR Data[a] for Fe(CO)$_2$(CNR)(R′-THPP) (4),[b] Fe(CO)$_2$(CNR)([2.2.2]bic) (7,8), *i*-Pr-THPP (9), and Ethenylpyrrole (10)

compd	^{13}C NMR data
4a	217.4 (ester *C*O), 213.5, 213.0 (*C*O), 175.8, 171.3, 166.0 (ester *C*O), 160.5 (*C*≡N-*t*-Bu), 158.4 (C=*C*—N), 93.8 (*C*=C—N), 84.7 (FeC=*C*—N), 71.0, 66.6 (bridgehead *C*), 55.5 (CN*C*(CH$_3$)$_3$), 53.2 (Fe*C*=C—N), 57.2, 55.0, 52.7, 52.3, 51.4, 51.8 (ester O*C*H$_3$, *C*H(CH$_3$)$_2$), 31.0 (CNC(*C*H$_3$)$_3$), 22.4, 20.0, 19.4, 18.6 (CH(*C*H$_3$)$_2$)
4b[c]	216.7 (ester *C*O), 212.2, 211.9 (*C*O), 172.2, 166.0, 164.6 (ester *C*O), 159.9 (C=*C*—N), 94.3, (*C*=C—N), 84.6 (FeC=*C*—N), 71.9, 67.5 (bridgehead *C*), 54.1 (Fe*C*=C—N), 56.3, 55.4, 53.5, 53.2, 51.9, 50.5 (ester OC*H*$_3$, *C*H(CH$_3$)$_2$), 51.2, 31.0, 19.2, 10.9 (*sec*-Bu *C*), 24.9, 23.1, 22.0, 20.9 (CH(*C*H$_3$)$_2$)
4c[c]	216.1 (ester *C*O), 212.3, 212.0 (*C*O), 170.9, 165.3, 166.4 (ester *C*O), 159.7 (C=*C*—N), 93.6 (*C*=C—N), 128.9, 128.5, 127.6, 127.3, 126.8, 124.9 (aryl *C*), 86.4 (FeC=*C*—N), 69.9, 66.8 (bridgehead *C*), 55.9 (Fe*C*=C—N), 55.4, 53.4, 52.8, 52.6, 51.6, 51.4 (ester O*C*H$_3$, *C*H(CH$_3$)$_2$), 48.3 (*C*H$_2$ aryl), 22.4, 21.8, 19.4, 18.3 (CH(*C*H$_3$)$_2$)
4d[c]	217.5 (ester *C*O), 214.2, 214.0 (*C*O), 175.9, 174.7, 172.5 (ester *C*O), 159.4 (C=*C*—N), 93.9 (*C*=C—N), 85.8 (FeC=*C*—N), 77.8, 67.3 (bridgehead *C*), 63.4 (N c-Hex *C*), 51.8 (Fe*C*=C—N), 55.9, 53.9, 53.4, 52.5, 52.1, 50.9, 46.2 (ester O*C*H$_3$, *C*H(CH$_3$)$_2$), 32.6, 24.6, 24.4 (c-Hex *C*), 23.05, 20.7, 20.1, 16.7 (CH(*C*H$_3$)$_2$)
4f[c]	215.8 (ester *C*O), 212.6, 212.0 (*C*O), 174.3, 172.8, 165.3 (ester *C*O), 157.9 (C=*C*—N), 134.9, 128.5, 127.7 (aryl *C*), 93.3 (*C*=C—N), 86.1 (FeC=*C*—N), 71.5, 68.0 (bridgehead *C*), 55.7 (Fe*C*=C—N), 55.3, 53.1, 52.8, 51.5, 51.4, 49.5 (ester O*C*H$_3$, *C*H(CH$_3$)$_2$), 22.6, 20.0, 19.4, 18.5 (CH(*C*H$_3$)$_2$)
4g[c]	217.1 (ester *C*O), 214.3, 214.0 (*C*O), 175.1, 171.9, 164.5 (ester *C*O), 158.8 (C=*C*—N), 93.8 (*C*=C—N), 85.1 (FeC=*C*—N), 71.6, 67.4 (bridgehead *C*), 64.4, 58.4 (N c-Hex *C*), 57.7 (CN*C*(CH$_3$)$_3$), 51.7 (Fe*C*=C—N), 53.4, 52.8, 51.7, 51.3 (ester O*C*H$_3$), 31.0 (CNC(*C*H$_3$)$_3$), 32.2, 29.6, 29.7, 26.7, 26.2, 25.5 (c-Hex *C*)
7e	211.0, 210.1 (*C*O), 209.8 (ring *C*=N aryl), 198.0, 127.0 (Fe—*C*=*C*), 178.4, 169.0 (ester *C*O), 170.3 (imine *C*=N), 172.8 (*C*≡N), 134.9, 134.8, 130.5, 130.4, 129.5, 129.4, 127.0, 126.9, 126.8, 126.5, 126.2 (aryl *C*), 64.5, 46.9 (*C*H(CH$_3$)$_2$), 62.3, 51.3 (ester O*C*H$_3$), 55.0 (N=C*C*), 18.4, 18.2 (aryl *C*H$_3$), 24.3, 23.4, 21.9, 19.0 (CH(*C*H$_3$)$_2$)
7f	209.7, 209.6 (*C*O), 209.4 (ring *C*=N aryl), 199.4, 126.9 (Fe—*C*=*C*), 179.0, 160.3 (ester *C*O), 169.1 (imine *C*=N), 174.1 (*C*≡N), 135.4, 135.2, 135.1, 134.9, 128.9, 128.8, 127.9, 127.8, 127.4, 127.3, 127.2, 127.0 (aryl *C*), 62.7, 41.5 (*C*H(CH$_3$)$_2$), 61.2, 51.5 (ester O*C*H$_3$), 53.8 (N=C*C*), 18.7, 18.6, 18.4, 18.2 (aryl *C*H$_3$), 23.7, 22.6, 22.3, 21.9 (CH(*C*H$_3$)$_2$)
8a	210.7, 209.9 (*C*O), 204.8 (ring *C*O), 200.6, 126.2 (Fe—*C*=*C*), 179.4, 160.7 (ester *C*O), 169.3 (*C*=N), 155.0 (*C*≡N), 64.3, 43.3 (*C*H(CH$_3$)$_2$), 64.2, 52.3 (ester O*C*H$_3$), 58.2 (CN*C*(CH$_3$)$_3$), 54.1 (N=C*C*), 30.6 (CNC(*C*H$_3$)$_3$), 24.1, 23.3, 22.4, 20.7 (CH(*C*H$_3$)$_2$)
8b[c]	217.0, 216.9, (*C*O), 212.9 (ring *C*O), 210.2, 125.7 (Fe—*C*=*C*), 179.9, 160.5 (ester O*C*H$_3$), 167.7 (*C*=N), 64.1, 41.7 (*C*H(CH$_3$)$_2$), 64.2, 52.0, (ester *C*O), 54.2 (N=C*C*), 51.9, 29.9, 21.6, 10.3 (*sec*-Bu *C*), 23.9, 23.8, 22.1, 20.7 (CH(*C*H$_3$)$_2$)
8c[c]	216.5, 213.3 (*C*O), 208.4 (ring *C*O), 200.4, 125.8 (Fe—*C*=*C*), 180.3, 164.2 (ester *C*O), 168.2 (*C*=N), 128.9, 128.7, 127.8, 126.7, 126.4, 125.8 (aryl *C*), 62.5, 41.9 (*C*H(CH$_3$)$_2$), 64.3, 52.7 (ester O*C*H$_3$), 53.7 (N=C*C*), 47.7 (*C*H$_2$ aryl), 23.9, 22.7, 22.1, 20.7 (CH(*C*H$_3$)$_2$)
8d	216.6, 214.6 (*C*O), 212.0 (ring *C*O), 201.0, 124.7 (Fe—*C*=*C*), 175.1, 165.3 (ester *C*O), 167.6 (*C*=N), 149.3 (*C*≡N), 63.2, 48.7 (*C*H(CH$_3$)$_2$), 62.2, 51.4 (ester O*C*H$_3$), 55.1 (N=C*C*), 45.5, 25.5, 24.7 (c-Hex *C*), 25.3, 24.2, 22.3, 19.9 (CH(*C*H$_3$)$_2$)
9	165.0, 164.4 (ester *CO*), 155.8 (C=*C*N), 95.7 (*C*=CN), 69.6 (bridgehead *C*), 53.4, 51.1, 49.3 (ester O*C*H$_3$, *C*H(CH$_3$)$_2$), 20.3, 20.2 (CH(*C*H$_3$)$_2$)
10	170.1, 164.9, 164.4, 163.5 (ester *C*O), 156.0 (C=*C*NH), 128.9, 127.3, 115.2, 111.1 (pyrrole *C*), 83.5 (*C*=CNH), 53.0, 52.7, 51.5, 51.1, 49.8, 48.2 (ester O*C*H$_3$, *C*H(CH$_3$)$_2$), 25.5, 24.3, 21.8, 21.5 (CH(*C*H$_3$)$_2$)

[a] The chemical shift values, in ppm relative to Me$_4$Si, were measured in CDCl$_3$ at 243 K and 75.47 MHz. [b] Only one of two signal sets is given. [c] The terminal isocyanide carbon atoms could not be observed.

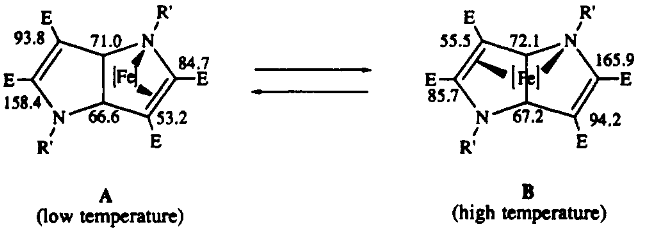

A (low temperature)

B (high temperature)

Figure 2. Coordination isomers of Fe(CO)$_2$(CNR)(THPP) (4).

Table VIII. IR Data[a] and Elemental Analyses of Fe(CO)$_2$(CNR)(R′-THPP) (4), Fe(CO)$_2$(CNR)([2.2.2]bic) (7, 8), *i*-Pr-THPP (9), and Ethenylpyrrole (10)

		elemental anal.[63] (%)		
compd	IR (cm^{-1})	C$_{obs}$ (C$_{calc}$)	H$_{obs}$ (H$_{calc}$)	N$_{obs}$ (N$_{calc}$)
4a	*2135*, 1991, 1941	52.09 (52.35)	5.93 (6.02)	6.62 (6.78)
4b	*2140*, 1995, 1940	53.01 (52.35)	5.95 (6.02)	6.93 (6.78)
4c	*2149*, 1990, 1935	53.30 (55.05)	5.28 (5.58)	5.82 (6.42)
4d	*2139*, 1990, 1941	52.48 (53.96)	6.49 (6.09)	6.32 (6.51)
4e	*2110*, 1993, 1946	54.01 (55.53)	6.11 (6.27)	5.47 (6.01)
4f	*2130*, 1990, 1935	55.69 (56.65)	6.64 (6.49)	6.12 (6.01)
7e	*2148*, 2030, 1986	59.24 (61.84)	5.85 (4.70)	8.86 (9.02)
7f	*2145*, 2030, 1987	not analysed		
8a	*2168*, 2036, 1985	51.86 (52.29)	6.27 (6.19)	8.01 (8.31)
8b	*2168*, 2030, 1988	49.53 (52.29)	6.35 (6.19)	7.72 (8.31)
8c	*2165*, 2035, 1992	not analysed		
8d	*2173*, 2038, 1984	53.28 (54.25)	6.93 (6.26)	6.96 (7.91)
9		55.13 (56.59)	6.58 (6.65)	6.51 (6.60)
10		55.20 (56.59)	6.55 (6.65)	6.49 (6.60)

[a] Stretching vibrations ν_{CO} and, *in italics*, ν_{CN}; recorded in CHCl$_3$ solution.

influence of the nearby cone angle becomes more significant when the substrate has to directly interact with the metal atom, e.g., in ligand substitution reactions.

Because in isocyanide complexes the substituents are located at a relatively large distance from the metal center, the remote cone angles of isocyanides are rather small compared to those of phosphines. The large distance also results in a comparatively large influence of the C≡N fragment on the nearby cone angle.

Table IX contains the results of the remote and nearby cone angle measurements for a wide variety of isocyanide ligands. This table demonstrates that in the nearby cone angle approach the influence of the terminal carbon atom dominates. As a consequence, it results in identical nearby cone angles for most of the isocyanides. When the remote cone angle is considered, on the other hand, there is an obvious difference between the different isocyanides. A point to emphasize is that not the absolute values but the relative ones should be taken into account. This is the logical consequence of the fact that the metal–isocyanide distance, which is variable for the different ligands, exerts an influence on the cone angle value. Consequently, it is the trend produced that is important.

In the literature, several reactions are known in which differences in reactivity are explained by the different steric properties of the isocyanide ligands in question. Most of these reactions concern isocyanide insertions.[43-48] It turned out that the smaller cyclohexyl isocyanide (remote cone angle 64°) reacted faster than the bulkier *tert*-butyl

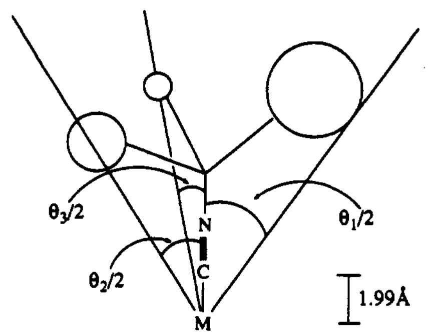

Figure 3. Method for measuring cone angles in $M{-}C{\equiv}N{-}C(R_1R_2R_3)$.

Table IX. Cone Angles of Isocyanides (CNR)

R	remote cone angle (deg)	nearby cone angle (deg)
CH_3	48	102
C_6H_5	57	102
m-CH_3-C_6H_3	57	102
C_2H_5	58	102
n-C_3H_7	58	102
n-C_4H_9	58	102
m-OCH_3-C_6H_4	60	102
m-$C(CH_3)_3$-C_6H_4	60	102
o-CH_3-C_6H_4	63	102
$CH_2(C_6H_5)$	63	102
c-C_6H_{11}	64	102
o-OCH_3-C_6H_4	64	102
$CH_2(SO_2)$(*p*-CH_3-C_6H_5)	64	102
$CH(CH_3)_2$	66	102
$CH(CH_3)(C_2H_5)$	67	102
2,6-$(CH_3)_2$-C_6H_3	69	102
CH_2(c-C_6H_{11})	70	106
o-$OC(CH_3)_3$-C_6H_4	71	108
o-$C(CH_3)_3$-C_6H_4	71	109
2,6-$(OCH_3)_2$-C_6H_3	71	102
$CH(CH_3)(C_6H_5)$	73	102
$C(CH_3)_3$	76	102
$CH(C_6H_5)_2$	79	102
2,6-$(C(CH_3)_3)_2$-C_6H_3	85	116
CH(c-C_6H_{11})$_2$	92	110
$C(C_6H_5)_3$	94	102
C(c-C_6H_{11})$_3$	114	114

isocyanide (remote cone angle 76°). Considering the fact that the insertion reaction directly involves the isocyano carbon atom, the nearby cone angle approach seems more logical to apply. The two nearby cone angles of the two isocyanides, however, are identical (102°) and therefore are unable to explain the difference in reactivity. This indicates that more research has to be done and more reactivity data on reactions with isocyanides are necessary. The presently available data do not support the validity of the nearby cone angle approach.

Scheme III. Isolobal Analogues

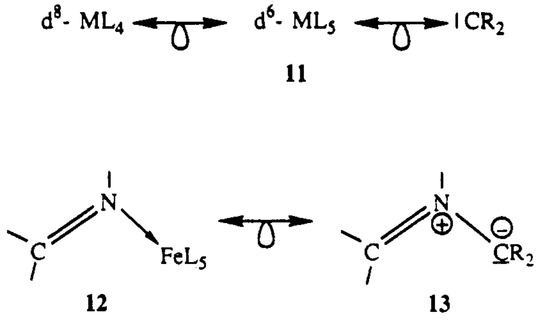

Yamamoto et al.[49] have estimated the bulk of isocyanide ligands. Irrespective of the different mean bond lengths and radii, they ended up with different results as a consequence of different suppositions. In our view they used the erroneous assumption that it is not possible to use the approach of half-angles (eq 1) to estimate the cone angles of unsymmetrical isocyanides. Instead, they used the definition of fan-shaped angles based upon the bulk of the isocyanide ligand in mutually perpendicular directions. Second, they postulated the substituents to be folded in such a way as to give a maximum angle. For the specific structural problem they described, the approach of fan-shaped angles proved to be useful, but from our point of view the values defined by Yamamoto et al. are not generally applicable.

Complex Formation. Formation of $Fe(CO)_2$(CNR)(R′-THPP) (4). If one bears in mind the isolobal analogy[50] of the Fe—N=C fragment and an azomethine ylide ($R_2C{=}N^+{-}C^-R_2$),[10e] the first step in the reaction (cf. Scheme II) can be looked upon as an oxidative [3 + 2] cycloaddition[51] of the alkyne to the 1,3-dipolar Fe—N=C fragment, leading to the formation of the ferrabicyclo[2.2.1] intermediate **7**. Although this intermediate in the reaction sequence cannot be isolated or detected, we have succeeded in the isolation and characterization of comparable structures. By addition of HBF_4 to the analogous compound formed from $Ru(CO)_3$(*i*-Pr-DAB) and DMAD the subsequent reaction steps could be prevented, and the N-protonated intermediate could be isolated and its structure determined by single-crystal X-ray diffraction.[1a] Also, in the analogous reaction of $Fe(CO)_3$(*p*-anisyl-DAB{Me,Me}), when $P(OMe)_3$ was used as an additional ligand, a bicyclo[2.2.1] complex was stabilized via a hydrogen bond to the nitrogen lone pair, as shown by a single-crystal X-ray structure.[10e]

The intermediate **2** has two options: it can either *intra*molecularly undergo an insertion reaction, leading to a bicyclic structure (**5** or **6**), or *inter*molecularly react with another alkyne molecule. This second reaction again can be described as a 1,3-dipolar oxidative [3 + 2] cycloaddition, by regarding **2** as a d^6-ML_5 fragment (**11**) with a coordinated imine unit. The five ligands at the iron(II) atom include two CO ligands, the CNR ligand, the amido nitrogen atom, and the former alkyne carbon atom. By using the isolobal analogy between d^6-ML_5 (**11**) and a carbene fragment, it is reasonable to formulate the second reaction of the alkyne in terms of a cycloaddition to the Fe—N=C fragment, because, as in the previously described[10] reaction of $Fe(CO)_3$(DAB), the isolobal relation **12**–**13** is applicable. The intermolecular reaction with DMAD leads to the formation of the intermediate **3**. At this point it is not clear whether the tricyclic structure **3**, which contains a seven-coordinated formal iron(IV) center, would have a definite lifetime or should be considered as

---

(43) Yamamoto, Y.; Yamazaki, H. *Bull. Chem. Soc. Jpn.* **1970**, *43*, 2653.

(44) Campagnaro, A.; Mantovani, A.; Uguagliati, P. *Inorg. Chim. Acta* **1985**, *99*, L15.

(45) Michelin, R. A.; Zanotto, L.; Braga, D.; Sabatino, P.; Angelici, R. J. *Inorg. Chem.* **1988**, *27*, 85.

(46) Yamamoto, Y.; Yamazaki, H. *J. Organomet. Chem.* **1970**, *24*, 717.

(47) Yamamoto, Y.; Yamazaki, H. *Inorg. Chem.* **1974**, *13*, 438.

(48) Ito, Y.; Hirao, T.; Ohta, N.; Saegusa, T. *Tetrahedron Lett.* **1977**, 1009.

(49) Yamamoto, Y.; Aoki, K.; Yamazaki, H. *Inorg. Chem.* **1979**, *18*, 1681.

(50) Hoffmann, R. *Angew. Chem.* **1982**, *94*, 725.

(51) (a) Huisgen, R. *Angew. Chem.* **1963**, *94*, 725. (b) Huisgen, R. *Angew. Chem.* **1963**, *75*, 742.

a transition state. In any case, however, it readily undergoes two successive reductive eliminations, leading to the formation of $Fe(CO)_2(CNR)(R'\text{-}THPP)$ (**9**).

The absence of this second cycloaddition in the reaction of $Fe(CO)_3(R'\text{-}DAB)$ is rationalized by electronic arguments. The substitution of CO by a better σ-donating/worse π-accepting[12] CNR ligand results in an enhanced electron density at the iron complex. As shown in a previous article,[14] concerning the synthesis and properties of the starting compounds $Fe(CO)_2(CNR)(R'\text{-}DAB)$ (**1**), the enhanced electron density is mainly reflected in the shift of the CO stretching vibrations to lower frequency. The ^{13}C NMR spectra also show a downfield shift for the CO ligands and an upfield shift of the imine carbon atoms of the DAB ligand, indicating an increase of electron density on the CO ligands and on the imine fragment. For the reactions of $Fe(CO)_3(R'\text{-}DAB)$ only alkynes with electron-withdrawing substituents proved to be reactive. This pointed to the fact that the Fe—N=C dipole can be described, according to the Sustmann classification,[52] as a HOMO-controlled or a nucleophilic dipole. This is confirmed by calculations for the isolobal azomethyne ylides, which revealed that they are electron-rich species with high HOMO and LUMO levels.[53] Also, preliminary CAS-SCF calculations on the present systems indicated high HOMO and LUMO levels.[54] Cycloadditions with a nucleophilic 1,3-dipole are characterized by a dominant interaction between the HOMO of the dipole and the LUMO of the dipolarophile. The reactivity of this type of cycloaddition reaction is enhanced by the introduction of electron-donating substituents on the dipole. Consequently, the introduction of an isocyanide ligand leads to an enhanced 1,3-dipolar activity.[55] Therefore, when a CO is replaced by the electron-donating CNR, the Fe^{II}—N=C unit in **2** is sufficiently activated to undergo a second cycloaddition. In the case of the reaction with $Fe(CO)_3(R'\text{-}DAB)$, only CO insertion takes place, leading to the bicyclic structure **8**, while the second Fe—N=C fragment remains intact.

Formation of the [2.2.2] Bicyclic Complex. Instead of a second cycloaddition, the intermediate **2** can also intramolecularly undergo an insertion reaction, resulting in the formation of the [2.2.2] bicyclic structure **5** or **6**. This insertion reaction, a nucleophilic attack of the nitrogen lone pair at the terminal carbon atom of the CO or CNR ligand, relieves strain in the one-atom nitrogen bridge of the [2.2.1] bicyclic structure.

In the literature, examples are known of competition between CO and CNR insertions.[12a,b,25b,56,57] A drawback is that most systems use the isocyanide as an incoming substrate instead of a coordinated ligand, and as a consequence conclusions about a competition are obscured by the preceding coordination reactions. The few examples known in which the starting complexes contain a CO as well as a CNR ligand show that when there is a choice within one molecule, isocyanide insertion prevails over CO insertion.[12a,b,25a,56] Isocyanide insertion leads to thermodynamically more stable compounds, although the activation energy is calculated to be higher (0.85 eV for CO compared to 1.8 eV for isocyanide).[12b,25a,56a,b,d,58]

To our knowledge, the present investigation is the first example in which both the electronic and the steric influences of the isocyanide ligands on the reaction have been thoroughly examined. For this study the following series of isocyanides has been used: *t*-Bu (**a**), *sec*-Bu (**b**), benzyl (**c**), *c*-Hex (**d**), and the aromatic *o*-tolyl (**e**) and 2,6-xylyl (**f**). We found that when the isocyanide bears an aliphatic group only CO insertion occurred, while in the case of the aromatic isocyanides only CNR-inserted complexes are found. This difference in behavior cannot be explained by steric properties, as can be concluded from Table IX. A good example is the comparison of *o*-tolyl isocyanide (**e**) and benzyl isocyanide (**c**), which have comparable steric properties but show an opposite insertion behavior. Obviously, this difference between the aromatic and the aliphatic isocyanides has to be explained electronically. The fact that aromatic isocyanides do give insertion whereas aliphatic ones do not is in accordance with the higher rate of insertion observed for aromatic isocyanides in the case of some platinum complexes ($[Pt(R')(CNR)(PR_3)_2]_x$).[59] The higher reactivity of aromatic isocyanides compared to aliphatic isocyanides has also been encountered in other studies.[45,60] The reason for this is that the electron-withdrawing phenyl groups[37] enhance the electrophilic character of the terminal isocyanide ligand; i.e., they make it more susceptible to nucleophilic attack of, in our case, the nitrogen lone pair. The fact that aromatic isocyanides are more susceptible to nucleophilic attack has also been observed for reactions with nucleophiles such as alcohols and amines.[12b,25a,44,45,61] The electron-donating aliphatic group diminishes the inclination to undergo insertion reactions, such that in this case CO insertion prevails.

Besides activation of the Fe—N=C fragment, the introduction of an isocyanide ligand also causes an activation of the two CO ligands toward insertion; the presence of the isocyanide ligands results in an enhanced π back-donation to the CO ligands, which makes them more electrophilic.[62] In spite of this enhanced CO reactivity, the complexes with aromatic isocyanides only give rise to isocyanide insertion. The trend for preferential

---

(52) (a) Sustmann, R. *Tetrahedron Lett.* **1971**, 2721. (b) Sustmann, R.; Trill, H. *Angew. Chem., Int. Ed. Engl.* **1972**, *11*, 838. (c) Sustmann, R. *Pure Appl. Chem.* **1974**, *40*, 569. (d) Fukui, K. *Acc. Chem. Res.* **1971**, *4*, 57. (e) Herndon, W. C. *Chem. Rev.* **1972**, *72*, 157. (f) Houk, K. N., Yamaguchi, K. In *1,3-Dipolar Cycloaddition Chemistry*; Padwa, A., Ed.; Wiley: New York, 1984; Chapter 13. (g) Bastide, J.; El Ghandour, N.; Henri-Rousseau, O. *Tetrahedron Lett.* **1972**, *41*, 4225.

(53) (a) Houk, K. N. *Acc. Chem. Res.* **1975**, *8*, 361. (b) Houk, K. N.; Sims, J.; Duke, R. E.; Strozier, R. W.; George, J. K. *J. Am. Chem. Soc.* **1973**, *95*, 7287. (c) Lown, J. W. In *1,3-Dipolar Cycloaddition Chemistry*; Padwa, A., Ed.; Wiley: New York, 1984; Chapter 6.

(54) Dedieu, A.; Liddell, M. J. To be submitted for publication.

(55) Although this enhanced 1,3-dipolar activity results in two cycloadditions of DMAD on both imine fragments, the system is not sufficiently activated to undergo cycloadditions with less reactive dipolarophiles such as alkenes.

(56) (a) Cardaci, G.; Bellachioma, G. *Polyhedron* **1983**, *2*, 967. (b) Berke, H.; Hoffmann, R. *J. Am. Chem. Soc.* **1978**, *100*, 7224. (c) Ashby, M. T.; Enemark, J. H. *Organometallics* **1987**, *6*, 1318. (d) Bellachioma, G.; Cardaci, G.; Macchioni, A.; Reichenbach, G. *Inorg. Chem.* **1992**, *31*, 63.

(57) Yamamoto, Y.; Yamazaki, H. *Inorg. Chem.* **1972**, *11*, 211.

(58) (a) Buller, I. S.; Basolo, F.; Pearson, R. G. *Inorg. Chem.* **1967**, *6*, 2074. (b) Adams, R. D.; Chodosh, D. F. *J. Am. Chem. Soc.* **1977**, *99*, 6544.

(59) Treichel, P. M.; Wagner, K. P.; Hess, R. W. *Inorg. Chem.* **1973**, *12*, 1471.

(60) (a) Dupont, J.; Pfeffer, M. *J. Chem. Soc., Dalton Trans.* **1990**, 3193. (b) Yamamoto, Y.; Yamazaki, H. *Inorg. Chim. Acta* **1980**, *41*, 229.

(61) (a) Boschi, T.; Crociani, B.; Nicolini, M.; Belluco, U. *Inorg. Chim. Acta* **1975**, *12*, 39. (b) Belluco, U.; Michelin, R. A.; Uguagliati, P. *J. Organomet. Chem.* **1983**, *250*, 565.

(62) It is known that more π back-donation leads to more positive polarization of the carbonyl C atom, thus making the carbonyl ligand more susceptible for nucleophilic attack. At first sight this seems counterintuitive, but it has been found that the calculated positive charges of the carbonyl C atoms decrease in the order $V(CO)_6^-$ (+0.25), $Cr(CO)_6$ (+0.20), and $Mn(CO)_6^+$ (+0.18); see: Caulton, K. G.; Fenske, R. F. *Inorg. Chem.* **1968**, *7*, 1273.

Scheme IV. Formation of Ethenylpyrrole 10

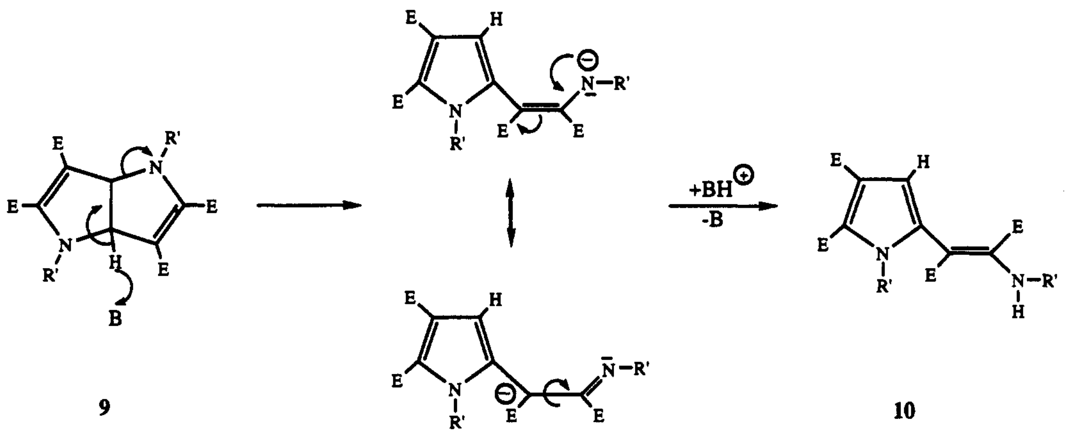

insertion appears to be aromatic isocyanides > CO > aliphatic isocyanides.

All bicyclo[2.2.2] complexes (**7**, **8**) contain a terminal isocyanide ligand. In **7**, the terminal isocyanide has been incorporated as an additional ligand L′ in a position trans to the inserted isocyanide. In **8**, it is the one already present in the starting complex **1** and, therefore, presumably in a position trans to the Fe–alkyne σ bond as in the analogous $P(OMe)_3$-containing complex.[10c] In the case of the aromatic isocyanide containing compounds **7e,f**, the additional isocyanide is still present in solution from the synthesis of the starting compounds **1**. In the case of the aliphatic isocyanide containing compounds **8a–d,g**, the additional CO was originally supplied by some decomposing **6**, resulting in a low yield of **8**. These yields increased after the reactions were carried out under an atmosphere of CO.

It proved to be impossible to isomerize the [2.2.2] bicyclic structures, via a reductive elimination and recoordination of the alkene double bond, to a 1,5-dihydropyrrol-2-one complex. This was not surprising, since it has already been known that the bicyclic complex **8**, with L′ equal to $P(OMe)_3$, also does not isomerize.[10] This was explained in terms of a stabilization by a donating ligand of the Fe(II) oxidation state and of the iron–carbon σ bonds, both disfavoring a reductive elimination.

THPP versus Bicyclo[2.2.2] Formation. Possible steric and/or electronic influences on the product distribution between **4** or **7** and **8** have to be discussed at the stage of intermediate **2**, where the reaction coordinate splits. Bulky isocyanides would hinder the approach of the second alkyne; i.e., an insertion reaction with the activated CO or aromatic isocyanide is preferred. However, the results indicate that steric influences, if present at all, are of minor importance in this reaction.

The complex distribution can be explained by electronic factors. The substitution of a CO by CNR results, as stated before, in increased activation of the Fe^{II}—N═C unit in intermediate **2** but also in an activation of the CO ligands. A part of **2** immediately reacts further with an alkyne to form intermediate **3**. This route is favored for the more electron donating aliphatic isocyanides (*t*-BuNC) because in those cases the Fe^{II}—N═C unit is highly activated. The other part of **2** gives rise to an insertion reaction. In the case of a complex with an aromatic isocyanide, this isocyanide preferentially inserts to give intermediate **5**.

Ethenylpyrrole Formation (10). The formation of ethenylpyrrole **10** from THPP **9** can be described by a base-catalyzed ring opening (cf. Scheme IV). In the first step, THPP **9** is deprotonated by a base, resulting in a ring-opening reaction. Subsequently the corresponding acid (HB^+) protonates the negatively charged nitrogen atom, to give the ethenylpyrrole **10**. During this reaction, most likely the THPP molecule **9** acts as a base.

Acknowledgment. Financial support from the Nederlandse organisatie voor Wetenschappelijk Onderzoek (NWO) and the stichting Scheikundig Onderzoek in Nederland (SON) is gratefully acknowledged. We are indebted to Dr. D. De Ridder and Drs. K. Goubitz for helpful discussions concerning the crystallographic section, to Ing. J.-M. Ernsting for practical assistance with the NMR experiments, to Ing. W. G. J. de Lange for the experimental HPLC section, and to H. Luyten for the manufacturing of the cone angle measurement device. Prof. Dr. P. W. N. M. van Leeuwen and Dr. C. J. Elsevier are thanked for fruitful discussions and advice.

Supplementary Material Available: Tables of fractional coordinates and isotropic thermal parameters for the hydrogen atoms, anisotropic thermal parameters for the non-hydrogen atoms, and all bond lengths and angles for the hydrogen atoms of **10** and Newman projections for **10** (10 pages). Ordering information is given on any current masthead page. Listings of the observed and calculated structure factors for **10** (30 pages) can be obtained from the authors.

OM920488F

---

(63) For presently unknown reasons, the isocyanide-containing complexes give notoriously bad elemental analyses, in particular for carbon. The deviations for compounds 9 and 10 have to be ascribed to the fact that they could hardly be obtained in crystalline form but mostly as sticky semisolids, which may retain some residual solvent molecules.